

This discussion paper is/has been under review for the journal Atmospheric Chemistry and Physics (ACP). Please refer to the corresponding final paper in ACP if available.

CCN activity of organic aerosols observed downwind of urban emissions during CARES

F. Mei^{1,*}, A. Setyan^{2,**}, Q. Zhang², and J. Wang¹

¹Brookhaven National Laboratory, Upton, New York, USA

²Department of Environmental Toxicology, University of California, Davis, California, USA

*now at: Pacific Northwest National Laboratory, Richland, Washington, USA

**now at: Ecole Nationale Supérieure des Mines de Douai, Département Chimie & Environnement, 941 rue Charles Bourseul, CS10838, 59508 Douai Cedex, France

Received: 23 February 2013 – Accepted: 20 March 2013 – Published: 9 April 2013

Correspondence to: J. Wang (jian@bnl.gov)

Published by Copernicus Publications on behalf of the European Geosciences Union.

9355

Abstract

During the Carbonaceous Aerosols and Radiative Effects Study (CARES), activation fraction of size-resolved aerosol particles and aerosol chemical composition were characterized at the T1 site (~60 km downwind of Sacramento, California) from 10 June to 28 June 2010. The hygroscopicity of CCN-active particles (κ_{CCN}) with diameter from 100 to 171 nm, derived from the size-resolved activated fraction, varied from 0.10 to 0.21, with an average of 0.15, which was substantially lower than that proposed for continental sites in earlier studies. The low κ_{CCN} value was due to the high organic volume fraction, averaged over 80 % at the T1 site. The derived κ_{CCN} exhibited little diurnal variation, consistent with the relatively constant organic volume fraction observed. At any time, over 90 % of the size selected particles with diameter between 100 and 171 nm were CCN active, suggesting most particles within this size range were aged background particles. Due to the large organic volume fraction, organic hygroscopicity (κ_{org}) strongly impacted particle hygroscopicity and therefore calculated CCN concentration. For vast majority of the cases, an increase of κ_{org} from 0.03 to 0.18, which are within the typical range, doubled the calculated CCN concentration. Organic hygroscopicity was derived from κ_{CCN} and aerosol chemical composition, and its variations with the fraction of total organic mass spectral signal at m/z 44 (f_{44}) and O:C were compared to results from previous studies. Overall, the relationships between κ_{org} and f_{44} are quite consistent for organic aerosol (OA) observed during field studies and those formed in smog chamber. Compared to the relationship between κ_{org} and f_{44} , the relationship between κ_{org} and O:C exhibits more significant differences among different studies, suggesting κ_{org} may be better parameterized using f_{44} . A least squares fit yielded $\kappa_{\text{org}} = 2.04 (\pm 0.07) \times f_{44} - 0.11 (\pm 0.01)$ with the Pearson R^2 value of 0.71. One possible explanation for the stronger correlation between κ_{org} and f_{44} is that the m/z 44 signal (mostly contributed by the CO_2^+ ion) is more closely related to organic acids, which may dominate the overall κ_{org} due to their relatively high water solubility and hygroscopicity.

9356

1 Introduction

Acting as cloud condensation nuclei (CCN), aerosol particles also indirectly affect the climate by changing the microphysical structure, lifetime, and coverage of clouds. An increase in aerosol concentration leads to a decrease of cloud droplet size and therefore enhancement of cloud albedo (Twomey, 1977). The smaller cloud droplet size resulting from the increased aerosol concentration also inhibits precipitation, leading to an increase in cloud lifetime and coverage (Albrecht, 1989). Although it is widely accepted that indirect effects of aerosols act to cool the Earth-atmosphere system by increasing cloud albedo, thickness, and coverage, the magnitudes of the effects are poorly understood. Currently, the indirect effects of aerosols remain the most uncertain components in forcing of climate change over the industrial period (IPCC, 2007).

Understanding aerosol indirect effects requires knowledge of the ability of aerosol particles to form cloud droplets at atmospherically relevant supersaturations (i.e., CCN activity).

The CCN activity of atmospheric particles can be effectively predicted using Köhler theory (Köhler, 1936), provided that the particle size and physicochemical properties of the solute, such as its molar volume, activity coefficient, and effect on surface tension are known (McFiggans et al., 2006). One key parameter that links the thermodynamic properties of aerosol species to their CCN activity, and eventually to aerosol indirect effects, is the hygroscopicity. Several essentially equivalent single parameter frameworks have been proposed to model the CCN activation and hygroscopicity of multi-component aerosols (Hudson and Da, 1996; Rissler et al., 2006; Petters and Kreidenweis, 2007; Wex et al., 2007; Petters and Kreidenweis, 2008). These single parameter frameworks combine many of the thermodynamic details necessary for the description of water activity, and provide a more streamlined approach to represent CCN activation in models. Here we use the hygroscopicity parameter κ proposed by Petters and Kreidenweis (2007, 2008), which can be conveniently derived from size-resolved CCN measurements. Besides droplet activation, hygroscopicity also describes particle

9357

growth under sub-saturated conditions and is derived from particle growth factor (GF) measured by Humidified Tandem Differential Mobility Analyzer (HTDMA). Previous studies suggest particles may exhibit larger κ values for droplet activation (derived from CCN measurements under supersaturated conditions) than that for particle growth (derived from particle GF under sub-saturated conditions) (Duplissy et al., 2008; Wex et al., 2008, 2009; Petters et al., 2009b; Good et al., 2010). In this paper, unless otherwise noted, “hygroscopicity” refers to κ associated with droplet activation under supersaturated conditions.

The hygroscopicities of ambient inorganic species are relatively well known. However, atmospheric aerosols often contain hundreds of organic species, which can contribute ~ 20 – 90 % to the total fine aerosol mass (Kanakidou et al., 2005; Zhang et al., 2007). Many studies have examined the CCN activity and hygroscopicity of organic aerosols, including laboratory generated organic aerosols with known composition (e.g., Raymond and Pandis, 2002; Kumar et al., 2003; Raymond and Pandis, 2003; Bilde and Svenningsson, 2004; Abbatt et al., 2005; Huff-Hartz et al., 2006; Svenningsson et al., 2006), secondary organic aerosols (SOA) generated in controlled environmental chambers, and aerosols generated in laboratory biomass burning experiments (e.g., Abbatt et al., 2005; Prenni et al., 2007; Duplissy et al., 2008, 2011; Asa-Awuku et al., 2009; King et al., 2009; Petters et al., 2009a; Lambe et al., 2011; Massoli et al., 2011). A number of field studies also reported the range of κ for the organic component of ambient aerosols (Shantz et al., 2008; Wang et al., 2008; Gunthe et al., 2009; Jimenez et al., 2009; Chang et al., 2010; Rose et al., 2010; Mei et al., 2013). Collectively, the laboratory and field studies suggest that organics have a fairly wide range of κ values ranging from 0 to 0.3, and κ_{org} can increase substantially during their chemical aging in the atmosphere (Jimenez et al., 2009; Duplissy et al., 2011; Lambe et al., 2011; Massoli et al., 2011; Mei et al., 2013).

The sensitivity of predicted CCN concentration and droplet number concentration to aerosol properties, including the hygroscopicity of organic species, are examined in a number of recent studies (Rissman et al., 2004; McFiggans et al., 2006; Wang, 2007;

9358

Wang et al., 2008; Reutter et al., 2009; Ervens et al., 2010; Kammermann et al., 2010; Ward et al., 2010). While these studies all recognize the importance of particle size distribution, mixing state, and volume fraction of organics in particles, they also indicate that the predicted CCN concentration and droplet number concentration can be sensitive to κ_{org} , and the value of κ_{org} needed to reproduce measured CCN concentration can vary substantially, and depends on the location and time of the study. Using constant κ for organic components may lead to significant biases in predicted CCN concentrations and aerosol indirect forcing (Liu and Wang, 2010). On the other hand, atmospheric aerosols often contain hundreds of organic species, and the hygroscopicities of many organic species are often not available. Therefore efficient parameterizations that can capture the major variation of κ_{org} are essential for implementation in large scale models. One promising idea is that the κ_{org} under both supersaturated and sub-saturated conditions may be parameterized based on the organic oxidation level (e.g., O : C atomic ratio), which can be measured by aerosol mass spectrometers (Aiken et al., 2008) and other techniques. For particle hygroscopic growth under sub-saturated conditions, measurements from TDMA show that κ_{org} increases with O : C for a number of organic aerosols (Jimenez et al., 2009; Duplissy et al., 2011). Positive correlations between κ_{org} and O : C were also found under supersaturated conditions for SOA and oxidized POA generated in a Potential Aerosol Mass (PAM) flow reactor (Massoli et al., 2010; Lambe et al., 2011), and ambient organic aerosols observed at rural (Chang et al., 2010) and urban (Mei et al., 2013) site. At present, the data on the hygroscopicity of ambient organics are scarce, and the relationship between κ_{org} and organic oxidation level needs to be examined for ambient aerosols from representative organic aerosol sources before it can be confidently implemented in climate models. In this paper we report particle hygroscopicity and mixing state derived from size-resolved CCN measurements carried out during CARES. The impact of κ_{org} on predicted CCN spectrum was examined. Organic hygroscopicity was derived from particle hygroscopicity and chemical composition and its relationship to organics oxidation level is discussed.

9359

2 Experimental method

2.1 Measurement site

The Carbonaceous Aerosol and Radiative Effects Study (CARES) was a field campaign focusing on the evolution of secondary organic and black carbon (BC) aerosols and their climate-related properties in the Sacramento urban plume as it was routinely transported into the forested Sierra Nevada foothills area (Zaveri et al., 2012). Aerosol measurements were taken from 2 June to 28 June 2010 at the T1 site, which was located about 60 km to the northeast of Sacramento in Cool, CA, a small town situated amidst a forested area rich in biogenic emissions (latitude: 38.87, longitude: -121.02 , altitude: ~ 460 m m.s.l.). The data related to the analysis presented in this paper were available from 10 June to 28 June. Aerosol data included aerosol size distribution, chemical composition, CCN spectrum (as a function of supersaturation), size-resolved CCN spectrum and activated fraction, all of which were taken at the ground level. All measurements are reported at ambient conditions and local time (UTC time minus 7 h) is used throughout this study.

2.2 Size resolved CCN spectrum and activated fraction

The size resolved CCN Spectrum and activated fraction were characterized by a scanning mobility particle sizer (SMPS) and a cloud condensation nuclei counter (CCN counter) operated in series (Frank et al., 2006; Petters et al., 2007; Moore et al., 2010). By isolating the influence from particle size, size-resolved CCN measurements provide unique insights into particle composition and mixing state, and their impacts on the particle CCN activity (Lance, 2007; Gunthe et al., 2009; Petters et al., 2009a; Asa-Awuku et al., 2010; Mochida et al., 2010; Padro et al., 2010, 2012; Rose et al., 2010; Irwin et al., 2011). The instrumentation setup is shown in Fig. 1. Ambient aerosol was first dried to below 20 % relative humidity and neutralized by a Kr-85 aerosol neutralizer (TSI, 3077A), and subsequently classified by a differential mobility analyzer (DMA, TSI

9360

3081). The classified aerosol was then simultaneously characterized by a condensation particle counter (CPC, TSI 3771) and a CCN counter (DMT, CCN-100) (Roberts and Nenes, 2005; Lance et al., 2006; Rose et al., 2008).

During CARES, the sample and sheath flows of the DMA were maintained at 0.8 and 8 L min⁻¹, respectively. The total flow of CPC3771 was reduced to 0.5 L min⁻¹ and the sample flow of the CCN counter was maintained at 0.3 L min⁻¹. The measurement sequence is illustrated in Fig. S1 (Supplement). The longitudinal temperature gradients of the CCN counter was stepped through 4.5, 5.5, 6.5, 8, 10, 12 °C (Fig. S1b), which corresponded to supersaturations (*S*) of 0.15 %, 0.19 %, 0.23 %, 0.30 %, 0.39 % and 0.45 %, respectively. The supersaturation inside the CCN counter was maintained at each value for approximately 40 min, during which the diameter of particles classified by the DMA was scanned between 20 nm and 350 nm eight times (310 s per scan) (Wang and Flagan, 1990). Immediately following each change of temperature gradient (i.e., supersaturation), the system waited for 100 s to ensure that all temperatures stabilized before the next scan of particle size commenced. The CCN counter was stepped through the above six *S* values approximately every 4 h. The aerosol size distribution was derived by inverting the particle concentration measured by the CPC using a routine described in Collins et al. (2002), which explicitly accounts for multiply-charged particles. The same procedure was also applied to measured CCN concentration to obtain size-resolved CCN concentration. The ratio of the two provided size-resolved CCN activated fraction (i.e., number fraction of particles that serve as CCN under the supersaturation as a function of particle size).

The CCN counter was calibrated for the 0.3 L min⁻¹ sampling flow rate, and under the six temperature gradients using ammonium sulfate at the CARES T1 site both before and after the study. The instrument supersaturations were derived from Köhler theory using a constant van't Hoff factor of 2.5 for ammonium sulfate. Since both sample pressure and temperature were essentially identical during measurements and calibrations, no correction of the calibrated supersaturation was necessary.

9361

2.3 Measurement of total CCN concentrations

In addition to size-resolved CCN spectrum and activated fraction, total CCN concentration was measured using a second DMT CCN counter operated at a flow rate of 0.3 L min⁻¹, and longitudinal temperature gradients of 4.0, 5.5, 6.6, 8.1, 10.3 °C. Based on calibrations using ammonium sulfate particles, the corresponding supersaturations derived from Köhler theory using a constant van't Hoff factor of 2.5 were 0.12 %, 0.20 %, 0.23 %, 0.30 %, 0.38 % for the five temperature gradients. The temperature gradient was stepped through the five values as shown in Fig. S1a. At each value, the temperature gradient was maintained for four minutes except for at 0.12 %, when an additional 10 min was included (i.e., total 14 min) because it took substantially longer time for temperatures to stabilize when the gradient was reduced from 10.3 °C to 4.0 °C. Data collected before temperatures had stabilized following changes of the temperature gradient were excluded from analysis. Same as size-resolved CCN measurements, both sampling pressure and temperature were practically identical between calibration and measurements.

2.4 Chemical composition

The concentrations of submicron non-refractory (NR-PM₁) organic and inorganic (nitrate, sulfate, ammonium, chloride) aerosol species were measured using a high resolution time-of-flight aerosol mass spectrometer (HR-ToF-AMS, Aerodyne Research Inc., hereinafter AMS for short) (DeCarlo et al., 2006). The AMS sampled from an inlet equipped with a PM₁ impactor (Brechtel Manufacturing Inc., Hayward, CA; model 8003). The ambient air passed through 3 feet of stainless steel tube with an inner diameter of 3/4 inch, 8 feet of copper tube with an inner diameter of 1/4 inch, 2 feet long temperature-controlled thermodenuder, and a Nafion dryer prior to sampling by the AMS. The resulting data was averaged over 2.5 min intervals. All data were analyzed using standard AMS software (SQUIRREL v1.51 and PIKA v1.10) within Igor Pro 6.2.2.2 (Wave Metrics, Lake Oswego, OR) (Sueper, 2011). Details of the AMS

9362

operation, data treatment, Positive Matrix Factorization (PMF) analysis, and data interpretation are given elsewhere (Setyan et al., 2012).

3 Data overview

Diurnal variations of aerosol properties observed from 10 June to 28 June 2010 are shown in Fig. 2, including aerosol particle size distribution (Fig. 2a), species mass concentrations measured by the AMS (Fig. 2b), derived volume fractions of major species (Fig. 2c), and measured CCN concentrations (Fig. 2d). Sulfate and nitrate were essentially neutralized by ammonium in the CCN-relevant sizes (Setyan et al., 2012). The volume fractions of major species were calculated using densities of organics (1.25 g cm⁻³), ammonium sulfate (1.77 g cm⁻³), ammonium nitrate (1.72 g cm⁻³), and BC (1.8 g cm⁻³). The mass concentration of BC was typically less than 0.1 μg m⁻³, contributing to less than 2% of the total submicron aerosol volume (not shown). High number concentration (N_{CN}) of Aitken mode particles was often observed in the afternoon between 12:00–18:00, and is attributed to early morning traffic-hour pollution transported from downtown Sacramento (Setyan et al., 2012). The mass concentration of sulfate and organics showed a relatively modest increase (~30% over otherwise nearly constant background) during this period. However, the species volume fractions were relatively constant during the day. Among all the species, organics had by far the largest contribution to the total submicron aerosol volume at ~85%. The contributions from sulfate and nitrate were only ~10% and ~5%, respectively. On average, CCN concentrations measured at 0.12% and 0.38% supersaturations were ~120 and ~1000 cm⁻³. No significant diurnal trends in measured CCN concentrations were observed, suggesting most particles transported from Sacramento area observed between 12:00–18:00 were not effective CCNs under measured supersaturations. This was likely due to the combination of the relatively small particle size (a majority of the particles transported to T1 during 12:00–18:00 were smaller than 50 nm in diameter)

9363

and particle compositions dominated by organics that in general are significantly less hygroscopic than inorganic salts such as sulfate.

4 Methods

4.1 Derivation of particle hygroscopicity and mixing state

Particle hygroscopicity κ and the mixing state were derived from the measured size-resolved CCN activated fraction using κ -Köhler theory (Petters and Kreidenweis, 2007). The same procedure was detailed in a previous study (Mei et al., 2013) and is briefly describe here. In κ -Köhler theory, the water vapor saturation ratio over an aqueous solution droplet S is given by:

$$S = \frac{D^3 - D_p^3}{D^3 - D_p^3(1 - \kappa)} \exp\left(\frac{4\sigma_w M_w}{RT \rho_w D}\right) \quad (1)$$

where D is the droplet diameter, D_p the dry diameter of the particle, M_w the molecular weight of water, σ_w the surface tension of pure water, ρ_w the density of water, R the gas constant, and T the absolute temperature. When κ is greater than 0.1, it can be conveniently derived as:

$$\kappa = \frac{4A^3}{27D_p^3 S_c^2} \quad (2)$$

where $A = \frac{4\sigma_w M_w}{RT \rho_w}$, and S_c is the particle critical supersaturation and was derived using the approach described below. Figure 3 shows an example of the activated fraction of size selected particles as a function of supersaturation. This example is for dry particles selected at 108 nm from 14:00 to 20:10 on 18 June. The activated fraction R_a , was

9364

near zero at the lowest supersaturation (0.15 %) measured. R_a increased with increasing supersaturation, and eventually reached a plateau of $\sim 92\%$. During CARES, the maximum activated fraction at the plateau, E , was often very close to 100 %. Occasionally, E is substantially less than 100 %, indicating external mixing of aerosol species for the size selected particles. For these cases, the difference $1 - E$ represents the number fraction of particles consisting of only non-hygroscopic species (e.g., BC) that cannot serve as CCN under typical atmospheric supersaturations.

The characteristic critical supersaturation (S^*) of the size selected CCN is represented by the supersaturation at which R_a reaches 50 % of E (Fig. 3). The slope of R_a with respect to supersaturation near S^* provides information on the heterogeneity of the composition for the size selected particles that are CCN active. For an ideal case when all CCN-active particles have the same composition and size, a step change of R_a from 0 to E would be observed as supersaturation increases and reaches S^* . A gradual increase in R_a suggests some of the particles have higher hygroscopicity and/or larger sizes (i.e., due to the resolution of DMA) and are able to activate at lower supersaturations than others. The activated fractions measured at the six supersaturations were fitted using both a sigmoid function (Lance, 2007; Bougiatioti et al., 2011; Cerully et al., 2011; Lance et al., 2012; Mei et al., 2013; Padro et al., 2012) and a lognormal function (Mei et al., 2013) (Supplement), with E and S^* among fitting parameters. For each set of measurements, the function form that yielded the best fit (i.e., smaller least square residue) was used for subsequent analysis. The probability density function of the hygroscopicity of size-selected CCN was first derived by differentiating the fitted R_a (as a function of S). The density function was then used to calculate the dispersion of CCN hygroscopicity. The dispersion of CCN hygroscopicity, which reflects the chemical heterogeneity of activated particles, is defined as $\sigma(\kappa)/\bar{\kappa}$, where $\sigma(\kappa)$ and $\bar{\kappa}$ are the standard deviation and the average of the CCN hygroscopicity, respectively. The details of the derivations are given in the Supplement.

9365

4.2 Derivation of organic hygroscopicity

Measurements from AMS show the composition of submicron particles was dominated by organics, followed by ammonium, sulfate, and nitrate. The contribution of chloride was negligible (i.e., below detection limit) especially for particles within the size range of size-revolved CCN measurements (Setyan et al., 2012). The analysis of anion and cation balance suggests that anionic species (NO_3^- , SO_4^{2-}) were neutralized by NH_4^+ over the relevant size range (Setyan et al., 2012). For refractory species, BC represented a negligible fraction of the total submicron aerosol volume (i.e. less than 2 %), and the contribution of sea salt and dust are also expected to be negligible for the size range of interest (i.e., less than 300 nm) at the T1 site. Therefore, aerosols within the size range examined were assumed consisting of the following three species: Organics, $(\text{NH}_4)_2\text{SO}_4$, and NH_4NO_3 . We note that a fraction of nitrate observed was organonitrate or metal nitrate. However, as nitrate only represented $\sim 3.5\%$ of total non-refractory PM1, assuming nitrate as NH_4NO_3 should not substantially affect derived κ_{org} values. During CARES, E observed at the T1 site was mostly very close to 100 % (the minimum E was 92 % during the periods chosen for deriving κ_{org} as described below). Therefore, particles were assumed as internal mixtures, and the particle hygroscopicity is therefore the volume average of the three participating species:

$$\kappa_{\text{CCN}} = \sum_i x_i \kappa_i = x_{\text{org}} \kappa_{\text{org}} + x_{(\text{NH}_4)_2\text{SO}_4} \kappa_{(\text{NH}_4)_2\text{SO}_4} + x_{\text{NH}_4\text{NO}_3} \kappa_{\text{NH}_4\text{NO}_3} \quad (3)$$

where x_i is the volume fraction of species i . The values of κ are 0.67 and 0.61 for $(\text{NH}_4)_2\text{SO}_4$ and NH_4NO_3 , respectively. The hygroscopicity of CCN (κ_{CCN}) can be derived from Eq. (2) based on S^* :

$$\kappa_{\text{CCN}} = \frac{4A^3}{27D_p^3(S^*)^2} \quad (4)$$

9366

and the organic hygroscopicity κ_{org} is given by subtracting the contribution of the other species from the overall CCN hygroscopicity:

$$\kappa_{\text{org}} = \frac{1}{X_{\text{org}}} \left(\kappa_{\text{CCN}} - \kappa_{\text{NH}_4\text{NO}_3} X_{\text{NH}_4\text{NO}_3} - \kappa_{(\text{NH}_4)_2\text{SO}_4} X_{(\text{NH}_4)_2\text{SO}_4} \right) \quad (5)$$

The derivation of κ_{org} requires the volume fraction of $(\text{NH}_4)_2\text{SO}_4$ and NH_4NO_3 of CCN at selected sizes, which were derived from size-resolved AMS measurements (particle time of flight “PToF” mode) as follows. AMS measurements were averaged into periods ranging from 7.6 to 14 h to increase signal-to-noise ratios (SNR). Particle chemical composition was essentially constant during these periods, which were identified using criteria described in Sect. 5.3. This averaging was especially necessary for size resolved mass concentrations and elemental ratios from AMS measurements because of both the low aerosol mass loading at the T1 site and the limited SNR arising from the low duty cycle during pToF measurements. Within the size range, species volume fractions at each size were derived from mass concentrations and densities of participating species. The densities of $(\text{NH}_4)_2\text{SO}_4$ and NH_4NO_3 were assumed to be 1770 kg m^{-3} and 1730 kg m^{-3} , respectively. Based on the O : C and O : H atomic ratios during the periods, organics were assumed to have a density of 1250 kg m^{-3} (Kuwata et al., 2012). The volume fractions required to derive κ_{org} from Eq. (5), were then calculated by combing the volume concentrations of organics, sulfate, and nitrate. In the derivation of species volume fractions at classified sizes, the particle vacuum aerodynamic diameter (D_{va} , measured by AMS) and particle mobility diameter (D_{m} , classified by DMA) were converted to particle volume equivalent diameter (D_{ve}) assuming spherical particles (for spherical particles, both D_{m} and D_{ve} are equal to particle geometric diameter). This assumption is reasonable for aged particles that are mixtures of organics, sulfate, and nitrate. In this study, κ_{org} was derived based on hygroscopicity of CCN classified at five sizes ranging from of 117 to 160 nm at which both the counting statistics of size-resolved CCN measurements (based on aerosol number) and the signal to noise ratio of the AMS measurements (aerosol mass based) were sufficient.

9367

4.3 Uncertainty analysis for organic hygroscopicity derivation

Based on Eq. (4), the uncertainty in derived κ_{org} can be attributed to the uncertainties in κ_{CCN} and species volume fractions of CCN. As the volume fractions were derived from volume concentrations computed from the AMS measurements, the uncertainty of derived κ_{org} is given by (detailed derivation described in the Supplement):

$$\sigma_{\kappa_{\text{org}}}^2 = \left(\frac{\kappa_{\text{CCN}}}{X_{\text{org}}} \right)^2 \left(\frac{\sigma_{\kappa_{\text{CCN}}}}{\kappa_{\text{CCN}}} \right)^2 + (\kappa_{\text{inorg}} - \kappa_{\text{org}})^2 (1 - x_{\text{org}})^2 \left[\left(\frac{\sigma_{v_{\text{org}}}}{v_{\text{org}}} \right)^2 + \left(\frac{\sigma_{v_{\text{inorg}}}}{v_{\text{inorg}}} \right)^2 \right] \quad (6)$$

where v_i represents the volume concentration of species i , and κ_{inorg} is the average hygroscopicity of the particle inorganic component, which included $(\text{NH}_4)_2\text{SO}_4$ and NH_4NO_3 :

$$\kappa_{\text{inorg}} = \frac{\kappa_{\text{NH}_4\text{NO}_3} X_{\text{NH}_4\text{NO}_3} + \kappa_{(\text{NH}_4)_2\text{SO}_4} X_{(\text{NH}_4)_2\text{SO}_4}}{X_{\text{NH}_4\text{NO}_3} + X_{(\text{NH}_4)_2\text{SO}_4}} \quad (7)$$

Note $(\text{NH}_4)_2\text{SO}_4$ and NH_4NO_3 have very similar κ values (0.67 and 0.61, respectively), for the derivation of the uncertainty in κ_{org} , a constant value of 0.64 was used for κ_{inorg} .

The first term on the right hand side (RHS) of Eq. (6) is associated with the uncertainty in derived κ_{CCN} (i.e., $\frac{\sigma_{\kappa_{\text{CCN}}}}{\kappa_{\text{CCN}}}$), which is due to the accuracy of the dry size of particles classified by the DMA (Wang et al., 2003) and S^* derived from size-resolved CCN measurements. This uncertainty was estimated ranging from 5% to 12% (Supplement). The second term on the RHS of Eq. (6) represents contributions due to the uncertainties in volume fractions of organics and inorganics (i.e., particle composition), derived from the mass concentrations measured by AMS and the densities of the species. For the purpose of estimating uncertainty in species volume fraction, an uncertainty of 10% was estimated for inorganics and organics volume concentrations, which were mainly due to the uncertainties in relative ionization efficiencies of AMS (Supplement).

9368

Equation (6) indicates that the contributions from $\sigma_{\kappa_{\text{CCN}}}$, $\sigma_{V_{\text{org}}}$, and $\sigma_{V_{\text{inorg}}}$ decreased with increasing x_{org} . These features are evident from the variation of $\sigma_{\kappa_{\text{org}}}^2$ and contributions from different terms as a function of x_{org} shown in Fig. 4. The variation in $\sigma_{\kappa_{\text{org}}}^2$ was calculated using Eq. (6) assuming 10% for $\frac{\sigma_{V_{\text{org}}}}{V_{\text{org}}}$ and $\frac{\sigma_{V_{\text{inorg}}}}{V_{\text{inorg}}}$, and 0.08 for κ_{org} . As shown later, the value of κ_{org} had very minor impact on $\sigma_{\kappa_{\text{org}}}^2$. $\frac{\sigma_{\kappa_{\text{CCN}}}}{\kappa_{\text{CCN}}}$ was assumed as 8%, which was representative for the measurements at the T1 site during CARES.

Figure 4 shows that the overall $\sigma_{\kappa_{\text{org}}}^2$, which was the combined contribution from $\sigma_{\kappa_{\text{CCN}}}$, $\sigma_{V_{\text{org}}}$ and $\sigma_{V_{\text{inorg}}}$ decreased rapidly with increasing x_{org} . This variation of $\sigma_{\kappa_{\text{org}}}^2$ with x_{org} can be explained as follows. First, at lower x_{org} , κ_{org} was increasingly being derived as the difference among three large numbers (Eqn. 5), which resulted in higher uncertainty in derived κ_{org} . Second, a higher x_{org} led to smaller uncertainty in derived x_{org} . For example, at x_{org} of 100% (i.e., pure OA particles), the uncertainty in measured organics mass concentration has no impact on derived x_{org} . This is also evident from Eq. (6), which shows that the contributions from $\sigma_{V_{\text{inorg}}}$ and $\sigma_{V_{\text{org}}}$ were scaled to $(1 - x_{\text{org}})^2$. Therefore, the analyses described below were focused on aerosols with organic volume fraction higher than 60%, at which overall uncertainty in derived κ_{org} was estimated to be less than 0.05 for the example presented in Fig. 4. Equation (6) suggests that the uncertainty weakly depends on the κ_{org} , because κ_{inorg} is typically much larger than κ_{org} , and the quantity $(\kappa_{\text{inorg}} - \kappa_{\text{org}})$ is insensitive to the value of κ_{org} . As a result, everything else being equal, we expect a larger relative uncertainty in κ_{org} for smaller κ_{org} values.

9369

5 Results

5.1 Hygroscopicity of activated particles

The hygroscopicity of size selected CCN with diameter between 100 and 171 nm ranged from 0.10 to 0.2, with an average of 0.15, in agreement with the results derived from CCN measurements over Sacramento valley onboard NOAA WP-3D during CalNex (Moore et al., 2012). The hygroscopicity range was substantially lower than that proposed for continental sites (Andreae and Rosenfeld, 2008), likely due to the higher volume fraction of organics. The hygroscopicity of size selected particles was averaged for sizes ranging from 100 to 171 nm, and its diurnal variation is shown in Fig. 5a. Median and mean hygroscopicities were essentially the same, and both showed a very narrow range from 0.13 to 0.16. There was no significant diurnal trend in the statistics of κ_{CCN} , consistent with relatively constant organic volume fraction during the day (Fig. 2). Figure 5b shows the diurnal variation of E , which represents the fraction of classified particles that were CCN-active. Unlikely earlier studies in urban environment (i.e., near major aerosol sources), where E decreased to $\sim 70\%$ or lower during morning traffic hours (Lance et al., 2012; Mei et al., 2013; Padro et al., 2012), the E observed at the T1 site was greater than 90% essentially at all time, suggesting vast majority particles within the 100–171 nm range were aged background particles. The average dispersion was 0.29, substantially lower than those observed in urban environment (Su et al., 2010; Padro et al., 2012). The lower value of dispersion reflects more aged aerosols observed at the T1 site, and is consistent with the finding that aerosol composition becomes increasingly more homogeneous as particles age through coagulation and condensation of secondary species (Wang et al., 2010; Mei et al., 2013). The diurnal variation showed lower dispersion in later morning and afternoon, and is attributed to stronger SOA production during the period and subsequent condensation on existing particles.

9370

5.2 Impact of organic hygroscopicity on calculated CCN concentration

The impact of κ_{org} on calculated CCN concentration (N_{CCN}) was examined using the following approach. CCN concentrations were calculated using four representative κ_{org} values, 0.03, 0.08, 0.13, and 0.18, which are within the typical range based on earlier laboratory studies (e.g., Prenni et al., 2007; Duplissy et al., 2008; Engelhart et al., 2008; Wex et al., 2009). Aerosol particles were assumed as internal mixtures, as suggested by the observed low hygroscopicity dispersion and close to unity E value for the size selected particles. Based on this assumption, particle hygroscopicity was derived as the volume average of the following three species: $(\text{NH}_4)_2\text{SO}_4$ and NH_4NO_3 and organics. On average, the aerosol mass concentration measured by the AMS at the T1 site peaked around 200 nm (vacuum aerodynamic diameter, ~ 160 nm for mobility or volume average diameter assuming spherical particles), and minor variation in organic volume fraction was observed from 100 to 200 nm (vacuum aerodynamic diameter), which corresponds to critical a supersaturation range of $\sim 0.14\%$ to $\sim 0.4\%$. Therefore, for the purpose of examining the sensitivity of calculated N_{CCN} to κ_{org} , particle hygroscopicity was computed from the bulk composition (i.e., derived from AMS MS mode measurements) using Eq. (3). Based on the particle hygroscopicity and κ -Köhler theory, the critical dry particle activation diameter (D_{pc}) was derived for the five supersaturations under which the total CCN concentrations were measured. The N_{CCN} at the five supersaturations were then computed from D_{pc} and the measured dry particle size distributions.

The comparison of calculated N_{CCN} and the measured at three supersaturations, 0.12%, 0.23%, and 0.38%, are shown in Fig. 6 (comparison at the other two supersaturations are similar and not shown). When x_{org} is greater than 90%, calculated N_{CCN} is very sensitive to κ_{org} value, especially at lower supersaturations. The ratio of calculated to measured N_{CCN} , derived through a bivariate least squares fit (i.e., orthogonal distance regression), increased from 0.75 by almost a factor of 2 to 2.08 when κ_{org} increased from 0.03 to 0.18. Each incremental increase of 0.05 in κ_{org} , which is

9371

well within the range of organic hygroscopicity reported in literature, led to ~ 40 – 50% increase in the calculated N_{CCN} . At the higher supersaturation of 0.38%, the difference between N_{CCN} calculated using the different κ_{org} values reduced somewhat to about a factor 2 (i.e. ratio increased from 0.58 to 1.10), but was still very significant. This reduced sensitivity was due to that a larger fraction of particle population was already CCN active at higher S . The sensitivity also strongly depends on the x_{org} . For example, when $80\% < x_{\text{org}} < 90\%$, N_{CCN} calculated at $S = 0.12\%$ increased by $\sim 100\%$ (i.e., ratio increased from 0.95 to 1.85) when κ_{org} increased from 0.03 to 0.18 compared to nearly a factor of 2 increase when x_{org} is greater than 90%, and the increase was further reduced to $\sim 40\%$ (i.e., the ratio increased from 1.14 to 1.52) when $70\% < x_{\text{org}} < 80\%$. For most of the measurements, the κ_{org} value required for an agreement between calculated and measured N_{CCN} ranged from 0.03 to 0.15, in agreement with κ_{org} derived from size-resolved CCN measurements described below.

During CARES, aerosols observed at the T1 site were dominated by organics. For the comparison described above, 24%, 54%, and 16% of the data points corresponded to $x_{\text{org}} > 90\%$, $80\% < x_{\text{org}} < 90\%$, and $70\% < x_{\text{org}} < 80\%$, respectively. Only 6% of data points were associated with x_{org} less than 70%. The decreasing sensitivity of the calculated N_{CCN} to κ_{org} is in agreement with earlier studies (e.g., Chang et al., 2007; Wang et al., 2008). When x_{org} is less than $\sim 60\%$, the overall hygroscopicity of internally mixed particles is dominated by inorganic species such as sulfate and nitrate, which have significantly higher κ values than organic compounds. As a result, the particle hygroscopicity, and therefore the calculated derived CCN concentration, is relatively insensitive to κ_{org} . When x_{org} reaches 80% or higher, the contribution of κ_{org} begins to dominate the overall particle hygroscopicity, and the value of κ_{org} strongly influences the calculated N_{CCN} . With stricter control of sulfur emission, aerosol organic fraction is likely to increase in the future. Therefore, simulated N_{CCN} will likely exhibit a stronger dependence on κ_{org} value when projecting future climate change. This again suggests the necessity of better understanding κ_{org} and its variation in the atmosphere for accurate prediction of N_{CCN} and aerosol indirect effects.

9372

5.3 κ_{org} derived from measurements at CARE T1 site and comparison with previous studies

To increase signal-to-noise ratio (SNR) and reduce the uncertainty in derived κ_{org} , we averaged measurements into periods during which particle chemical composition essentially remained constant. These periods, ranging from 7.6 to 14 h, were identified using the following criteria:

1. The variation in bulk organic volume fraction (i.e., the difference between the maximum and minimum) was less than 10 % during the averaging period. This criterion was to ensure essentially constant particle composition, and therefore hygroscopicity, during the periods such that data could be averaged to increase signal to noise ratio or counting statistics.
2. The average bulk organic volume fraction was no less than 60 % during the period, as the uncertainty in derived κ_{org} increased rapidly with decreasing x_{org} (Fig. 5).

A total of 18 periods were identified using the above criteria. During these periods, E is greater than 96 %, and $\sigma(\kappa)/\bar{\kappa}$ is less than 0.3, indicating the assumption of internally mixed particles was mostly appropriate. As described earlier, for each period, the analysis focused on 5 sizes ranging from 117 nm to 160 nm, where both the counting statistics of size-resolved CCN measurements (based on aerosol number) and the signal to noise ratio of the AMS measurements (aerosol mass based) were sufficient. κ_{org} derived from these cases ranged from 0.04 to 0.11 with an average value of 0.08, within the ranges observed in earlier studies (e.g., Hersey et al., 2011). These values are also in agreement with results from earlier smog chamber studies, which showed the hygroscopicity ranged from 0.04 to 0.14 for secondary organic aerosol formed from both biogenic and anthropogenic VOC precursors (Prenni et al., 2007; Duplissy et al., 2008; Engelhart et al., 2008; Wex et al., 2009).

9373

5.4 Relationship between κ_{org} and organic oxidation level

The relationship between derived κ_{org} and f_{44} , which is the fraction of total organic mass signal at m/z 44, is shown in Fig. 7a. The m/z 44 signal is due mostly to acids (Takegawa et al., 2007; Duplissy et al., 2011) or acid-derived species, such as esters, and f_{44} is closely related to the organic oxidation level (i.e., O : C ratio) (Aiken et al., 2008). The uncertainty of derived κ_{org} was calculated using the approach described earlier. The precision of f_{44} derived from measurements by the same AMS was estimated as 3 % (relative variation, Aiken et al., 2008), and the inter-instrument variability for f_{44} is about 10 % (relative variation, Ng et al., 2010). As the results are compared to earlier studies during which f_{44} was also derived from AMS measurements, the uncertainty in derived f_{44} was estimated as 10 % (Hayes et al., 2012). Also included in Fig. 7 are results based on similar analysis of the measurements carried out at the LA supersite during CalNex from 15 May to 4 June 2010 (Mei et al., 2013). The LA supersite was principally a receptor site for pollution from downtown LA, and SOA was a major aerosol component at the site (Hayes et al., 2012). Overall, the dependences of κ_{org} on f_{44} are in agreement for organic aerosols observed at the T1 site and the CalNex-LA site. Based on results from both sites, a least squares fit taking into consideration of uncertainties in both derived κ_{org} and f_{44} yielded $\kappa_{\text{org}} = 2.04 (\pm 0.07) \times f_{44} - 0.11 (\pm 0.01)$. The Pearson R^2 was 0.71, suggesting most of the variation in κ_{org} observed at the two sites can be explained by the variation in f_{44} alone.

The variation of κ_{org} was also examined as a function of organic oxidation level (i.e., O : C atomic ratio) as was done in earlier studies, and the result is shown in Fig. 7b. For both sites, O : C of size selected CCN was calculated from size-resolved f_{44} using the specific relationship between O : C and f_{44} , which was characterized using the bulk O : C and f_{44} derived from MS mode data collected at each site. This is an adaptation of the technique described by Aiken et al. (2008). The relationships were O : C = $3.99 \times f_{44}$ and O : C = $3.25 \times f_{44}$ for organic aerosols observed at the T1 site during CARES (i.e., this study) and the LA site during CalNex, respectively (Hayes et al., 2012; Setyan et

9374

al., 2012). The uncertainty in derived O : C was similarly estimated as 10%. Whereas overall κ_{org} exhibited an increasing trend with increasing O : C, as reported in earlier studies, the value of κ_{org} derived from this study was statistically lower than that derived from data collected at CalNex LA site when O : C ranges from 0.35 to 0.45. A least square fit of κ_{org} vs. O : C yielded $\kappa_{\text{org}} = 1.00 (\pm 0.02) \times (\text{O} : \text{C}) - 0.28 (\pm 0.01)$ with a significantly lower R^2 value of 0.41, suggesting that κ_{org} may be better parameterized by f_{44} than O : C.

The relationships between κ_{org} and f_{44} and between κ_{org} and O : C are compared to earlier studies described below (Fig. 8). Duplissy et al. (2011) reported κ_{org} (under sub-saturated conditions) derived from the GF of SOA formed from 1,3,5-trimethylbenzene (TMB), a surrogate for anthropogenic precursors, and SOA formed from representative biogenic precursors including isoprene and α -pinene in a smog chamber. Also included in the comparison are the results derived from the GF of organic aerosols measured in the Mexico City and at the high-alpine site Jungfraujoch, Switzerland (Duplissy et al., 2011). Using size-resolved CCN measurements, Massoli et al. (2010) and Lambe et al. (2011) examined the hygroscopicity of SOA and oxidized POA (OPOA) formed from the oxidation of a range of precursors representing atmospherically relevant biogenic and anthropogenic sources. The SOA and OPOA particles were generated via controlled exposure of precursors to OH radicals and/or O_3 in a Potential Aerosol Mass (PAM) flow reactor over timescales equivalent to 1–20 days of atmospheric aging resulting in O : C ratios ranging from 0.05 to 1.42. Chang et al. (2010) derived κ_{org} based on CCN measurements at a rural site in Ontario, Canada.

The results from Massoli et al. (2010) was not included in Fig. 8a because f_{44} values were not available. Overall, results from different studies showed quite consistent relationships between κ_{org} and f_{44} . For example, the relationship derived from this study and the measurements at the CalNex-LA site showed good agreement with those of ambient organic aerosols observed in Mexico City and at the high-alpine site Jungfraujoch. At the same f_{44} , κ_{org} of SOA formed from TMB in a smog chamber was substantially higher than those of SOA formed from isoprene and α -pinene. One possible

9375

explanation is that for SOA formed from TMB photooxidation, the acids present in the aerosol are mainly mono-acids, while the acids found in the SOA from α -pinene or isoprene photooxidation are approximately half mono- and half di-acids (Duplissy et al., 2011). At a given f_{44} value, κ_{org} of ambient organic aerosol observed at the CARES T1 site, CalNex-LA site, Mexico City, and Jungfraujoch was mostly between those of SOA formed from TMB and α -pinene or isoprene in the smog chamber, possibly because ambient SOA were formed from both anthropogenic and biogenic precursors. Chang et al. (2010) reported similar κ_{org} values at low f_{44} around 0.08–0.10, but a steeper increase of κ_{org} with increasing f_{44} when compared to κ_{org} observed in this study and at the CalNex-LA site. Because κ_{org} was derived from total CCN measurement (i.e., not size-resolved) in Chang et al. (2010), the relatively large uncertainty may partially explain some of the differences. For OA generated in PAM reactors, κ_{org} overlapped with those derived from field measurements when f_{44} ranges from 0.12 to 0.14, but exhibited a substantially weaker dependence on f_{44} .

All studies showed that κ_{org} generally increases with increasing O : C. However, compared to the relationship between κ_{org} and f_{44} , the relationship between κ_{org} and O : C exhibits more significant differences among the studies. For example, at O : C ratio of 0.5, κ_{org} derived in different studies ranged from ~ 0.1 to ~ 0.2 . For the results from Duplissy et al. (2011) and Chang et al. (2010), the differences may be partially due to the uncertainty in derived O : C values. At present, AMS data analysis software only allows derivation of bulk O : C through analysis of high resolution mass spectral obtained during the MS mode operation. This approach was employed by Massoli et al. (2010) and Lambe et al. (2011) to derive the bulk O : C, which should represent O : C at various CCN sizes in their studies, because no substantial O : C dependence on particle size is expected for organic aerosols formed in the PAM reactor. For this study and Mei et al. (2013), O : C of organics at CCN sizes was derived from size-resolved f_{44} using the relationship between O : C and f_{44} , which was characterized using the bulk O : C and f_{44} derived from MS mode data collected at each site. This approach was also employed to derive O : C from f_{44} for some of the results presented in Lambe et al. (2011).

9376

Therefore, we expect O : C values derived in this study, Lambe et al. (2011), and Mei et al. (2013) are reasonably accurate. Chang et al. (2010) and Duplissy et al. (2011) derived O : C using the relationship between O : C and f_{44} reported in an earlier study (Aiken et al., 2008), which might not be completely accurate for the aerosols observed in their studies.

Similar to the relationship between κ_{org} and f_{44} , κ_{org} of OA generated in PAM reactor (Lambe et al., 2011; Massoli et al., 2011) exhibited a weaker dependence on O : C than those derived from this study and Mei et al. (2013). At O : C values greater than 0.5, κ_{org} reported by Massoli et al. (2010) and Lambe et al. (2011) were substantially lower than those derived from field measurements (Mei et al., 2013). The organic mass loading examined by Massoli et al. (2010) ranged from 1 to 100 $\mu\text{g m}^{-3}$, which encompasses the typical range of ambient OA mass loading. In addition, the relationship between κ_{org} and O : C reported by Massoli et al. (2010) exhibited little dependence on organic mass loading. Therefore the differences in the relationship between κ_{org} and O : C among the studies could not be explained by the variations in organic mass loading, and may be due to the differences in organics composition between ambient organic aerosols and those formed in PAM reactors. For example, the formation of SOA proceeds under “low NO_x” chemistry in PAM reactor because NO_x is quickly oxidized to HNO₃. However, ambient SOA may form under different NO_x conditions, especially in urban environment (e.g. at CalNex-LA site). In addition, the concentrations of oxidants inside PAM are several orders of magnitude higher than typically observed in the ambient atmosphere, which may potentially lead to different compounds in the SOA formed. Cloud processing and aqueous chemistry in wet aerosols may also contribute substantially to SOA formation, while SOA are mainly formed through gas phase reactions in smog chamber or PAM reactor. This may also lead to different SOA composition and therefore the relationship between κ_{org} and O : C. However, it is worth noting that the relationship between κ_{org} and f_{44} for SOA formed in a smog chamber (Duplissy et al., 2011) is quite consistent with that derived from some of the field studies (Fig. 7a). These discrepancies suggest that more results on κ_{org} of ambient aerosols are needed

9377

to better understand and represent organic hygroscopicity in climate models, and future studies are needed to verify and understand the differences in κ_{org} between ambient OA and those formed in PAM reactors shown in Fig. 7.

Organic aerosols may exhibit a range of relationships between f_{44} and O : C, as evidenced by the differences among the relationships observed at the T1 site, the CalNex-LA site (Hayes et al., 2012), and those reported in previous studies (e.g., Aiken et al., 2008). The more consistent relationship between κ_{org} and f_{44} for different studies (Fig. 8a) and the higher R^2 value for the linear regression of κ_{org} on f_{44} (Fig. 7a) suggest that κ_{org} may be better parameterized using f_{44} than O : C. The better correlation between κ_{org} and f_{44} could be due to the following reasons. One key determinant of the hygroscopicity of organic compound is its water solubility. For typical ambient particles that are mixtures of both organic and inorganic species, organics with solubility less than $\sim 5 \times 10^{-4}$ have negligible contribution to CCN activation (i.e., negligible contribution to derived κ_{org}), whereas organics with solubility greater than ~ 0.05 are completely dissolved at the point of activation (Petters and Kreidenweis, 2008). Here the solubility is defined as the volume of solute per unit volume of water present in a saturated solution. The CO₂⁺ (m/z 44) is due mostly to acids (Duplissy et al., 2011) or acid-derived species, such as esters. Organic acids typically have larger solubility in water, therefore may contribute significantly to the overall κ_{org} . Other oxygenated compounds in organic aerosol such as aldehydes may have much lower solubility, and therefore negligible contribution to the derived κ_{org} if the solubility is less than $\sim 5 \times 10^{-4}$. This may explain the stronger correlation between κ_{org} and f_{44} , which is closely related to the fraction of organic acids. It is worth noting that non-acid compounds such as methyl tetrols identified in SOA formed from Isoprene also have high water solubility. However, these compounds may contribute to only a small fraction of the total organic aerosols, especially for those formed under high NO_x condition (e.g., Edney et al., 2005). Currently, the identity and the solubility of many organic compounds in atmospheric aerosols are not known, and data on κ_{org} for ambient aerosol are still very limited. Future measurements

9378

- Engelhart, G. J., Asa-Awuku, A., Nenes, A., and Pandis, S. N.: CCN activity and droplet growth kinetics of fresh and aged monoterpene secondary organic aerosol, *Atmos. Chem. Phys.*, 8, 3937–3949, doi:10.5194/acp-8-3937-2008, 2008.
- 5 Ervens, B., Cubison, M. J., Andrews, E., Feingold, G., Ogren, J. A., Jimenez, J. L., Quinn, P. K., Bates, T. S., Wang, J., Zhang, Q., Coe, H., Flynn, M., and Allan, J. D.: CCN predictions using simplified assumptions of organic aerosol composition and mixing state: a synthesis from six different locations, *Atmos. Chem. Phys.*, 10, 4795–4807, doi:10.5194/acp-10-4795-2010, 2010.
- 10 Frank, G. P., Dusek, U., and Andreae, M. O.: Technical note: A method for measuring size-resolved CCN in the atmosphere, *Atmos. Chem. Phys. Discuss.*, 6, 4879–4895, doi:10.5194/acpd-6-4879-2006, 2006.
- Good, N., Topping, D. O., Allan, J. D., Flynn, M., Fuentes, E., Irwin, M., Williams, P. I., Coe, H., and McFiggans, G.: Consistency between parameterisations of aerosol hygroscopicity and CCN activity during the RHaMBLe discovery cruise, *Atmos. Chem. Phys.*, 10, 3189–3203, doi:10.5194/acp-10-3189-2010, 2010.
- 15 Gunthe, S. S., King, S. M., Rose, D., Chen, Q., Roldin, P., Farmer, D. K., Jimenez, J. L., Artaxo, P., Andreae, M. O., Martin, S. T., and Pöschl, U.: Cloud condensation nuclei in pristine tropical rainforest air of Amazonia: size-resolved measurements and modeling of atmospheric aerosol composition and CCN activity, *Atmos. Chem. Phys.*, 9, 7551–7575, doi:10.5194/acp-9-7551-2009, 2009.
- 20 Hayes, P. L., Ortega, A. M., Cubison, M. J., Froyd, K. D., Zhao, Y., Cliff, S. S., Hu, W. W., Toohey, D. W., Flynn, J. H., Lefer, B. L., Grossberg, N., Alvarez, S., Rappenglück, B., Taylor, J. W., Allan, J. D., Holloway, J. S., Gilman, J. B., Kuster, W. C., Gouw, J. A. d., Massoli, P., Zhang, X., Liu, J., Weber, R. J., Corrigan, A. L., Russell, L. M., Isaacman, G., Worton, D. R., Kreisberg, N. M., Hering, S. V., Goldstein, A. H., Thalman, R., Waxman, E. M., Volkamer, R., Lin, Y. H., Surratt, J. D., Kleindienst, T. E., Offenberg, J. H., Dusanter, S., Griffith, S., Stevens, P. S., Brioude, J., Angevine, W. M., and Jimenez, J. L.: Aerosol Composition and Sources in Los Angeles during the 2010 CalNex Campaign, *J. Geophys. Res.*, submitted, 2012.
- 25 Hersey, S. P., Craven, J. S., Schilling, K. A., Metcalf, A. R., Sorooshian, A., Chan, M. N., Flagan, R. C., and Seinfeld, J. H.: The Pasadena Aerosol Characterization Observatory (PACO): chemical and physical analysis of the Western Los Angeles basin aerosol, *Atmos. Chem. Phys.*, 11, 7417–7443, doi:10.5194/acp-11-7417-2011, 2011.
- 30

9383

- Hudson, J. G. and Da, X. Y.: Volatility and size of cloud condensation nuclei, *J. Geophys. Res.*, 101, 4435–4442, 1996.
- Huff-Hartz, K. E. H., Tischuk, J. E., Chan, M. N., Chan, C. K., Donahue, N. M., and Pandis, S. N.: Cloud condensation nuclei activation of limited solubility organic aerosol, *Atmos. Environ.*, 5 40, 605–617, 2006.
- IPCC: Climate Change 2007 – The Physical Science Basis: Contribution of Working Group I to the Fourth Assessment Report of the IPCC, Cambridge University Press, New York, 2007.
- 10 Irwin, M., Robinson, N., Allan, J. D., Coe, H., and McFiggans, G.: Size-resolved aerosol water uptake and cloud condensation nuclei measurements as measured above a Southeast Asian rainforest during OP3, *Atmos. Chem. Phys.*, 11, 11157–11174, doi:10.5194/acp-11-11157-2011, 2011.
- 15 Jimenez, J. L., Canagaratna, M. R., Donahue, N. M., Prevot, A. S. H., Zhang, Q., Kroll, J. H., DeCarlo, P. F., Allan, J. D., Coe, H., Ng, N. L., Aiken, A. C., Docherty, K. S., Ulbrich, I. M., Grieshop, A. P., Robinson, A. L., Duplissy, J., Smith, J. D., Wilson, K. R., Lanz, V. A., Hueglin, C., Sun, Y. L., Tian, J., Laaksonen, A., Raatikainen, T., Rautiainen, J., Vaattovaara, P., Ehn, M., Kulmala, M., Tomlinson, J. M., Collins, D. R., Cubison, M. J., Dunlea, E. J., Huffman, J. A., Onasch, T. B., Alfarra, M. R., Williams, P. I., Bower, K., Kondo, Y., Schneider, J., Drewnick, F., Borrmann, S., Weimer, S., Demerjian, K., Salcedo, D., Cottrell, L., Griffin, R., Takami, A., Miyoshi, T., Hatakeyama, S., Shimono, A., Sun, J. Y., Zhang, Y. M., Dzepina, K., Kimmel, J. R., Sueper, D., Jayne, J. T., Herndon, S. C., Trimborn, A. M., Williams, L. R., Wood, E. C., Middlebrook, A. M., Kolb, C. E., Baltensperger, U., and Worsnop, D. R.: Evolution of Organic Aerosols in the Atmosphere, *Science*, 326, 1525–1529, 2009.
- 20 Kammermann, L., Gysel, M., Weingartner, E., Herich, H., Cziczo, D. J., Holst, T., Svenningsson, B., Arneth, A., and Baltensperger, U.: Subarctic atmospheric aerosol composition: 3. Measured and modeled properties of cloud condensation nuclei, *J. Geophys. Res.*, 115, D04202, doi:10.1029/2009JD012447, 2010.
- 25 Kanakidou, M., Seinfeld, J. H., Pandis, S. N., Barnes, I., Dentener, F. J., Facchini, M. C., Van Dingenen, R., Ervens, B., Nenes, A., Nielsen, C. J., Swietlicki, E., Putaud, J. P., Balkanski, Y., Fuzzi, S., Horth, J., Moortgat, G. K., Winterhalter, R., Myhre, C. E. L., Tsigaridis, K., Vignati, E., Stephanou, E. G., and Wilson, J.: Organic aerosol and global climate modelling: a review, *Atmos. Chem. Phys.*, 5, 1053–1123, doi:10.5194/acp-5-1053-2005, 2005.
- 30

9384

- King, S. M., Rosenoern, T., Shilling, J. E., Chen, Q., and Martin, S. T.: Increased cloud activation potential of secondary organic aerosol for atmospheric mass loadings, *Atmos. Chem. Phys.*, 9, 2959–2971, doi:10.5194/acp-9-2959-2009, 2009.
- Köhler, H.: The nucleus in and the growth of hygroscopic droplets, *Trans. Farad. Soc.*, 32, 1152–1161, 1936.
- Pradeep Kumar, P., Broekhuizen, K., and Abbatt, J. P. D.: Organic acids as cloud condensation nuclei: Laboratory studies of highly soluble and insoluble species, *Atmos. Chem. Phys.*, 3, 509–520, doi:10.5194/acp-3-509-2003, 2003.
- Kuwata, M., Zorn, S. R., and Martin, S. T.: Using Elemental Ratios to Predict the Density of Organic Material Composed of Carbon, Hydrogen, and Oxygen, *Environ. Sci. Technol.*, 46, 787–794, 2012.
- Lambe, A. T., Onasch, T. B., Massoli, P., Croasdale, D. R., Wright, J. P., Ahern, A. T., Williams, L. R., Worsnop, D. R., Brune, W. H., and Davidovits, P.: Laboratory studies of the chemical composition and cloud condensation nuclei (CCN) activity of secondary organic aerosol (SOA) and oxidized primary organic aerosol (OPOA), *Atmos. Chem. Phys.*, 11, 8913–8928, doi:10.5194/acp-11-8913-2011, 2011.
- Lance, S., Medina, J., Smith, J. N., and Nenes, A.: Mapping the operation of the DMT Continuous Flow CCN counter, *Aerosol Sci. Technol.*, 40, 242–254, 2006.
- Lance, S.: Quantifying compositional impacts of ambient aerosol on cloud droplet formation, Ph.D., Georgia Institute of Technology, Atlanta, 2007.
- Lance, S., Raatikainen, T., Onasch, T., Worsnop, D. R., Yu, X.-Y., Alexander, M. L., Stolzenburg, M. R., McMurry, P. H., Smith, J. N., and Nenes, A.: Aerosol mixing-state, hygroscopic growth and cloud activation efficiency during MIRAGE 2006, *Atmos. Chem. Phys. Discuss.*, 12, 15709–15742, doi:10.5194/acpd-12-15709-2012, 2012.
- Liu, X. and Wang, J.: How important is organic aerosol hygroscopicity to aerosol indirect forcing?, *Environ. Res. Lett.*, 5, 044010, doi:10.1088/1748-9326/5/4/044010, 2010.
- Massoli, P., Lambe, A. T., Ahern, A. T., Williams, L. R., Ehn, M., Mikkilä, J., Canagaratna, M. R., Brune, W. H., Onasch, T. B., Jayne, J. T., Petaja, T., Kulmala, M., Laaksonen, A., Kolb, C. E., Davidovits, P., and Worsnop, D. R.: Relationship between aerosol oxidation level and hygroscopic properties of laboratory generated secondary organic aerosol (SOA) particles, *Geophys. Res. Lett.*, 37, L24801, doi:10.1029/2010GL045258, 2010.
- Massoli, P., Lambe, A. T., Ahern, A. T., Williams, L. R., Ehn, M., Mikkilä, J., Canagaratna, M. R., Brune, W. H., Onasch, T. B., Jayne, J. T., Petaja, T., Kulmala, M., Laaksonen, A., Kolb,

9385

- C. E., Davidovits, P., and Worsnop, D. R.: Relationship between aerosol oxidation level and hygroscopic properties of laboratory generated secondary organic aerosol (SOA) particles, *Geophys. Res. Lett.*, 38, L24801, doi:10.1029/2011GL046687, 2011.
- McFiggans, G., Artaxo, P., Baltensperger, U., Coe, H., Facchini, M. C., Feingold, G., Fuzzi, S., Gysel, M., Laaksonen, A., Lohmann, U., Mentel, T. F., Murphy, D. M., O'Dowd, C. D., Snider, J. R., and Weingartner, E.: The effect of physical and chemical aerosol properties on warm cloud droplet activation, *Atmos. Chem. Phys.*, 6, 2593–2649, doi:10.5194/acp-6-2593-2006, 2006.
- Mei, F., Hayes, P. L., Ortega, A. M., Taylor, J. W., Allan, J. D., Gilman, J. B., Kuster, W. C., de Gouw, J. A., Jimenez, J. L., and Wang, J.: Droplet activation properties of organic aerosols observed at an urban site during CalNex-LA, *J. Geophys. Res.*, in press, 2013.
- Mochida, M., Nishita-Hara, C., Kitamori, Y., Aggarwal, S. G., Kawamura, K., Miura, K., and Takami, A.: Size-segregated measurements of cloud condensation nucleus activity and hygroscopic growth for aerosols at Cape Hedo, Japan, in spring 2008, *J. Geophys. Res.*, 115, D21207, doi:10.1029/2009JD013216, 2010.
- Moffet, R. C. and Prather, K. A.: In-situ measurements of the mixing state and optical properties of soot with implications for radiative forcing estimates, *Proc. Natl. Acad. Sci. USA*, 106, 11872–11877, 2009.
- Moore, R. H., Nenes, A., and Medina, J.: Scanning Mobility CCN Analysis-A Method for Fast Measurements of Size-Resolved CCN Distributions and Activation Kinetics, *Aerosol Sci. Technol.*, 44, 861–871, doi:10.1080/02786826.2010.498715, 2010.
- Moore, R. H., Cerully, K., Bahreini, R., Brock, C. A., Middlebrook, A. M., and Nenes, A.: Hygroscopicity and composition of California CCN during summer 2010, *J. Geophys. Res.*, 117, D00V12, doi:10.1029/2011JD017352, 2012.
- Ng, N. L., Canagaratna, M. R., Zhang, Q., Jimenez, J. L., Tian, J., Ulbrich, I. M., Kroll, J. H., Docherty, K. S., Chhabra, P. S., Bahreini, R., Murphy, S. M., Seinfeld, J. H., Hildebrandt, L., Donahue, N. M., DeCarlo, P. F., Lanz, V. A., Prévôt, A. S. H., Dinar, E., Rudich, Y., and Worsnop, D. R.: Organic aerosol components observed in Northern Hemispheric datasets from Aerosol Mass Spectrometry, *Atmos. Chem. Phys.*, 10, 4625–4641, doi:10.5194/acp-10-4625-2010, 2010.
- Padro, L. T., Tkacik, D., Lathem, T., Hennigan, C. J., Sullivan, A. P., Weber, R. J., Huey, L. G., and Nenes, A.: Investigation of cloud condensation nuclei properties and droplet growth

9386

- kinetics of the water-soluble aerosol fraction in Mexico City, *J. Geophys. Res.*, 115, D09204, doi:10.1029/2009JD013195, 2010.
- Padró, L. T., Moore, R. H., Zhang, X., Rastogi, N., Weber, R. J., and Nenes, A.: Mixing state and compositional effects on CCN activity and droplet growth kinetics of size-resolved CCN in an urban environment, *Atmos. Chem. Phys.*, 12, 10239–10255, doi:10.5194/acp-12-10239-2012, 2012.
- Petters, M. D. and Kreidenweis, S. M.: A single parameter representation of hygroscopic growth and cloud condensation nucleus activity, *Atmos. Chem. Phys.*, 7, 1961–1971, doi:10.5194/acp-7-1961-2007, 2007.
- Petters, M. D., Prenni, A. J., Kreidenweis, S. M., and DeMott, P. J.: On measuring the critical diameter of cloud condensation nuclei using mobility selected aerosol, *Aerosol Sci. Technol.*, 41, 907–913, 2007.
- Petters, M. D. and Kreidenweis, S. M.: A single parameter representation of hygroscopic growth and cloud condensation nucleus activity – Part 2: Including solubility, *Atmos. Chem. Phys.*, 8, 6273–6279, doi:10.5194/acp-8-6273-2008, 2008.
- Petters, M. D., Carrico, C. M., Kreidenweis, S. M., Prenni, A. J., DeMott, P. J., Collett, J. L., and Moosmuller, H.: Cloud condensation nucleation activity of biomass burning aerosol, *J. Geophys. Res.*, 114, D22205, doi:10.1029/2009JD012353, 2009a.
- Petters, M. D., Wex, H., Carrico, C. M., Hallbauer, E., Massling, A., McMeeking, G. R., Poulain, L., Wu, Z., Kreidenweis, S. M., and Stratmann, F.: Towards closing the gap between hygroscopic growth and activation for secondary organic aerosol – Part 2: Theoretical approaches, *Atmos. Chem. Phys.*, 9, 3999–4009, doi:10.5194/acp-9-3999-2009, 2009b.
- Prenni, A. J., Petters, M. D., Kreidenweis, S. M., DeMott, P. J., and Ziemann, P. J.: Cloud droplet activation of secondary organic aerosol, *J. Geophys. Res.*, 112, D10223, doi:10.1029/2006JD007963, 2007.
- Raymond, T. M. and Pandis, S. N.: Cloud activation of single-component organic aerosol particles, *J. Geophys. Res.*, 107, 4787, doi:10.1029/2002JD002159, 2002.
- Raymond, T. M. and Pandis, S. N.: Formation of cloud droplets by multicomponent organic particles, *J. Geophys. Res.*, 108, 4469, doi:10.1029/2003JD003503, 2003.
- Reutter, P., Su, H., Trentmann, J., Simmel, M., Rose, D., Gunthe, S. S., Wernli, H., Andreae, M. O., and Pöschl, U.: Aerosol- and updraft-limited regimes of cloud droplet formation: influence of particle number, size and hygroscopicity on the activation of cloud condensation nuclei (CCN), *Atmos. Chem. Phys.*, 9, 7067–7080, doi:10.5194/acp-9-7067-2009, 2009.

9387

- Riemer, N., Vogel, H., and Vogel, B.: Soot aging time scales in polluted regions during day and night, *Atmos. Chem. Phys.*, 4, 1885–1893, doi:10.5194/acp-4-1885-2004, 2004.
- Riemer, N., West, M., Zaveri, R. A., and Easter, R. C.: Simulating the evolution of soot mixing state with a particle-resolved aerosol model, *J. Geophys. Res.*, 114, D09202, doi:10.1029/2008JD011073, 2009.
- Rissler, J., Vestin, A., Swietlicki, E., Fisch, G., Zhou, J., Artaxo, P., and Andreae, M. O.: Size distribution and hygroscopic properties of aerosol particles from dry-season biomass burning in Amazonia, *Atmos. Chem. Phys.*, 6, 471–491, doi:10.5194/acp-6-471-2006, 2006.
- Rissman, T. A., Nenes, A., and Seinfeld, J. H.: Chemical amplification (or dampening) of the Twomey effect: Conditions derived from droplet activation theory, *J. Atmos. Sci.*, 61, 919–930, 2004.
- Roberts, G. C. and Nenes, A.: A continuous-flow streamwise thermal-gradient CCN chamber for atmospheric measurements, *Aerosol Sci. Technol.*, 39, 206–221, 2005.
- Rose, D., Gunthe, S. S., Mikhailov, E., Frank, G. P., Dusek, U., Andreae, M. O., and Pöschl, U.: Calibration and measurement uncertainties of a continuous-flow cloud condensation nuclei counter (DMT-CCNC): CCN activation of ammonium sulfate and sodium chloride aerosol particles in theory and experiment, *Atmos. Chem. Phys.*, 8, 1153–1179, doi:10.5194/acp-8-1153-2008, 2008.
- Rose, D., Nowak, A., Achtert, P., Wiedensohler, A., Hu, M., Shao, M., Zhang, Y., Andreae, M. O., and Pöschl, U.: Cloud condensation nuclei in polluted air and biomass burning smoke near the mega-city Guangzhou, China – Part 1: Size-resolved measurements and implications for the modeling of aerosol particle hygroscopicity and CCN activity, *Atmos. Chem. Phys.*, 10, 3365–3383, doi:10.5194/acp-10-3365-2010, 2010.
- Setyan, A., Zhang, Q., Merkel, M., Knighton, W. B., Sun, Y., Song, C., Shilling, J. E., Onasch, T. B., Herndon, S. C., Worsnop, D. R., Fast, J. D., Zaveri, R. A., Berg, L. K., Wiedensohler, A., Flowers, B. A., Dubey, M. K., and Subramanian, R.: Characterization of submicron particles influenced by mixed biogenic and anthropogenic emissions using high-resolution aerosol mass spectrometry: results from CARES, *Atmos. Chem. Phys.*, 12, 8131–8156, doi:10.5194/acp-12-8131-2012, 2012.
- Shantz, N. C., Leaitch, W. R., Phinney, L., Mozurkewich, M., and Toom-Saunty, D.: The effect of organic compounds on the growth rate of cloud droplets in marine and forest settings, *Atmos. Chem. Phys.*, 8, 5869–5887, doi:10.5194/acp-8-5869-2008, 2008.

9388

- Su, H., Rose, D., Cheng, Y. F., Gunthe, S. S., Massling, A., Stock, M., Wiedensohler, A., Andreae, M. O., and Pöschl, U.: Hygroscopicity distribution concept for measurement data analysis and modeling of aerosol particle mixing state with regard to hygroscopic growth and CCN activation, *Atmos. Chem. Phys.*, 10, 7489–7503, doi:10.5194/acp-10-7489-2010, 2010.
- 5 Svenningsson, B., Rissler, J., Swietlicki, E., Mircea, M., Bilde, M., Facchini, M. C., Decesari, S., Fuzzi, S., Zhou, J., Mønster, J., and Rosenørn, T.: Hygroscopic growth and critical super-saturations for mixed aerosol particles of inorganic and organic compounds of atmospheric relevance, *Atmos. Chem. Phys.*, 6, 1937–1952, doi:10.5194/acp-6-1937-2006, 2006.
- Takegawa, N., Miyakawa, T., Kawamura, K., and Kondo, Y.: Contribution of selected dicarboxylic and omega-oxocarboxylic acids in ambient aerosol to the m/z 44 signal of an aerodyne aerosol mass spectrometer, *Aerosol Sci. Technol.*, 41, 418–437, doi:10.1080/02786820701203215, 2007.
- ToF-AMS Analysis Software: http://cires.colorado.edu/jimenez-group/wiki/index.php/ToF-AMS_Analysis_Software, 2011.
- 15 Twomey, S.: Influence of Pollution on Shortwave Albedo of Clouds, *J. Atmos. Sci.*, 34, 1149–1152, 1977.
- Wang, J., Flagan, R. C., and Seinfeld, J. H.: A differential mobility analyzer (DMA) system for submicron aerosol measurements at ambient relative humidity, *Aerosol Sci. Technol.*, 37, 46–52, 2003.
- 20 Wang, J.: Effects of spatial and temporal variations in aerosol properties on mean cloud albedo, *J. Geophys. Res.*, 112, D16201, doi:10.1029/2007JD008565, 2007.
- Wang, J., Lee, Y.-N., Daum, P. H., Jayne, J., and Alexander, M. L.: Effects of aerosol organics on cloud condensation nucleus (CCN) concentration and first indirect aerosol effect, *Atmos. Chem. Phys.*, 8, 6325–6339, doi:10.5194/acp-8-6325-2008, 2008.
- 25 Wang, J., Cubison, M. J., Aiken, A. C., Jimenez, J. L., and Collins, D. R.: The importance of aerosol mixing state and size-resolved composition on CCN concentration and the variation of the importance with atmospheric aging of aerosols, *Atmos. Chem. Phys.*, 10, 7267–7283, doi:10.5194/acp-10-7267-2010, 2010.
- Wang, S. C. and Flagan, R. C.: Scanning Electrical Mobility Spectrometer, *Aerosol Sci. Technol.*, 13, 230–240, 1990.
- 30 Ward, D. S., Eidhammer, T., Cotton, W. R., and Kreidenweis, S. M.: The role of the particle size distribution in assessing aerosol composition effects on simulated droplet activation, *Atmos. Chem. Phys.*, 10, 5435–5447, doi:10.5194/acp-10-5435-2010, 2010.

9389

- Wex, H., Hennig, T., Salma, I., Ocskay, R., Kiselev, A., Henning, S., Massling, A., Wiedensohler, A., and Stratmann, F.: Hygroscopic growth and measured and modeled critical super-saturations of an atmospheric HULIS sample, *Geophys. Res. Lett.*, 34, L02818, doi:10.1029/2006GL028260, 2007.
- 5 Wex, H., Stratmann, F., Topping, D., and McFiggans, G.: The Kelvin versus the Raoult Term in the Kohler Equation, *J. Atmos. Sci.*, 65, 4004–4016, 2008.
- Wex, H., Petters, M. D., Carrico, C. M., Hallbauer, E., Massling, A., McMeeking, G. R., Poulain, L., Wu, Z., Kreidenweis, S. M., and Stratmann, F.: Towards closing the gap between hygroscopic growth and activation for secondary organic aerosol: Part 1 – Evidence from measurements, *Atmos. Chem. Phys.*, 9, 3987–3997, doi:10.5194/acp-9-3987-2009, 2009.
- 10 Zaveri, R. A., Shaw, W. J., Cziczo, D. J., Schmid, B., Ferrare, R. A., Alexander, M. L., Alexandrov, M., Alvarez, R. J., Arnott, W. P., Atkinson, D. B., Baidar, S., Banta, R. M., Barnard, J. C., Beranek, J., Berg, L. K., Brechtel, F., Brewer, W. A., Cahill, J. F., Cairns, B., Cappa, C. D., Chand, D., China, S., Comstock, J. M., Dubey, M. K., Easter, R. C., Erickson, M. H., Fast, J. D., Floerchinger, C., Flowers, B. A., Fortner, E., Gaffney, J. S., Gilles, M. K., Gorkowski, K., Gustafson, W. I., Gyawali, M., Hair, J., Hardesty, R. M., Harworth, J. W., Herndon, S., Hiranuma, N., Hostetler, C., Hubbe, J. M., Jayne, J. T., Jeong, H., Jobson, B. T., Kassianov, E. I., Kleinman, L. I., Kluzek, C., Knighton, B., Kolesar, K. R., Kuang, C., Kubátová, A., Langford, A. O., Laskin, A., Laulainen, N., Marchbanks, R. D., Mazzoleni, C., Mei, F., Moffet, R. C., Nelson, D., Obland, M. D., Oetjen, H., Onasch, T. B., Ortega, I., Ottaviani, M., Pekour, M., Prather, K. A., Radney, J. G., Rogers, R. R., Sandberg, S. P., Sedlacek, A., Senff, C. J., Senum, G., Setyan, A., Shilling, J. E., Shrivastava, M., Song, C., Springston, S. R., Subramanian, R., Suski, K., Tomlinson, J., Volkamer, R., Wallace, H. W., Wang, J., Weickmann, A. M., Worsnop, D. R., Yu, X.-Y., Zelenyuk, A., and Zhang, Q.: Overview of the 2010 Carbonaceous Aerosols and Radiative Effects Study (CARES), *Atmos. Chem. Phys.*, 12, 7647–7687, doi:10.5194/acp-12-7647-2012, 2012.
- 15 s Zhang, Q., Jimenez, J. L., Canagaratna, M. R., Allan, J. D., Coe, H., Ulbrich, I., Alfarra, M. R., Takami, A., Middlebrook, A. M., Sun, Y. L., Dzepina, K., Dunlea, E., Docherty, K., DeCarlo, P. F., Salcedo, D., Onasch, T., Jayne, J. T., Miyoshi, T., Shimono, A., Hatakeyama, S., Takegawa, N., Kondo, Y., Schneider, J., Drewnick, F., Borrmann, S., Weimer, S., Demerjian, K., Williams, P., Bower, K., Bahreini, R., Cottrell, L., Griffin, R. J., Rautiainen, J., Sun, J. Y., Zhang, Y. M., and Worsnop, D. R.: Ubiquity and dominance of oxygenated species in organic aerosols in
- 30

9390

9391

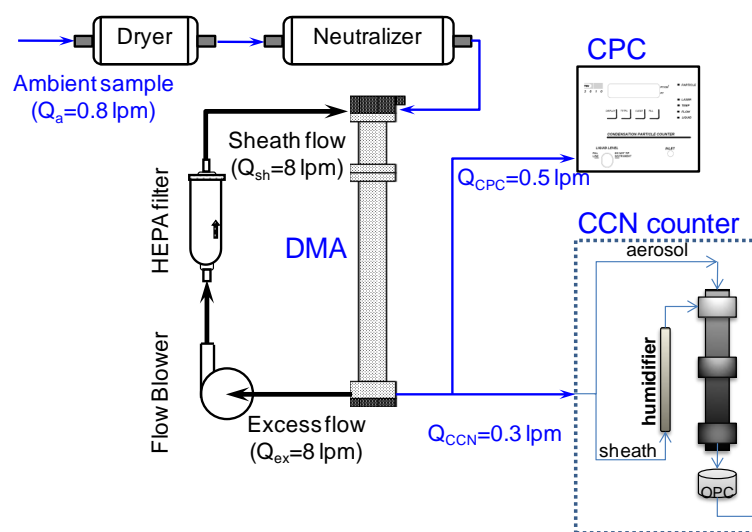


Fig. 1. Setup of the size-resolved CCN spectrum and activated fraction measurements.

9392

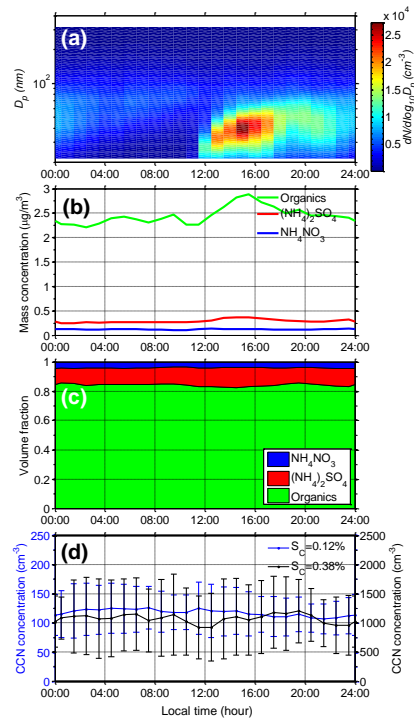


Fig. 2. Diurnal variations of aerosol properties observed at the T1 site from 10 to 28 June 2012. **(a)** Aerosol size distribution measured by SMPS; **(b)** mass concentrations and **(c)** volume fractions of organics, (NH₄)₂SO₄, and NH₄NO₃; and **(d)** CCN concentrations measured at supersaturations of 0.12% and 0.38%.

9393

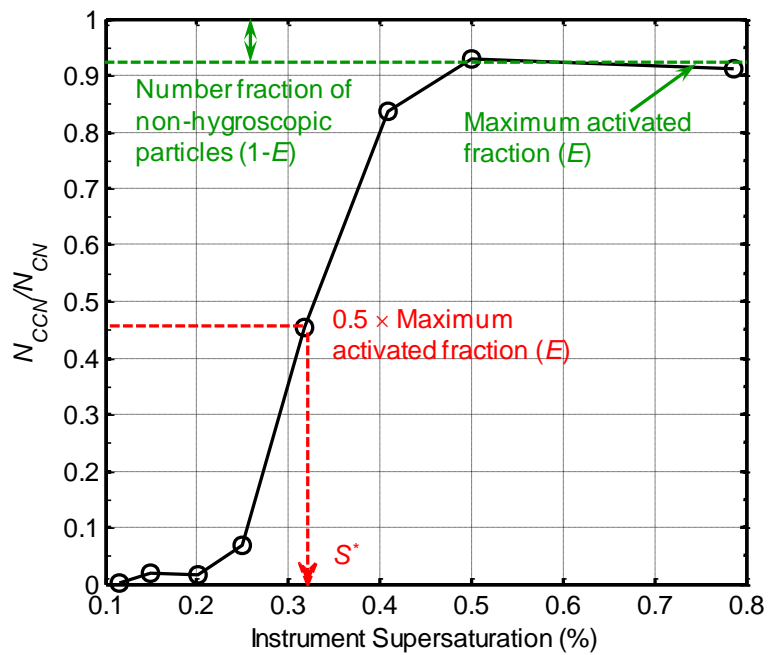


Fig. 3. Activated fraction as a function of supersaturation for particles classified at 108 nm averaged from 14:00 to 20:10 on 18 June.

9394

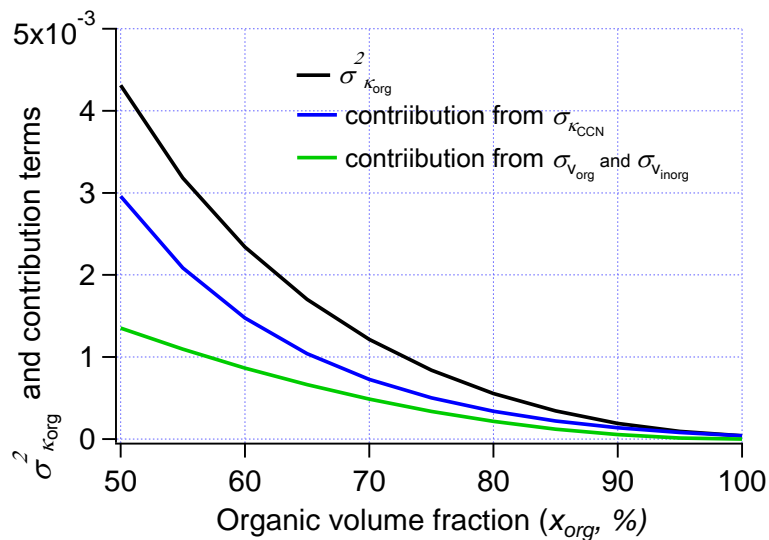


Fig. 4. Variations of $\sigma_{K_{org}}^2$ and contributions from different terms as functions of x_{org} . The value of $\sigma_{K_{org}}^2$ was calculated using Eq. (6) assuming 10% for $\frac{\sigma_{V_{org}}}{V_{org}}$ and $\frac{\sigma_{V_{inorg}}}{V_{inorg}}$, and 0.08 for $K_{org} \cdot \frac{\sigma_{K_{CCN}}}{K_{CCN}}$ was assumed as 8%.

9395

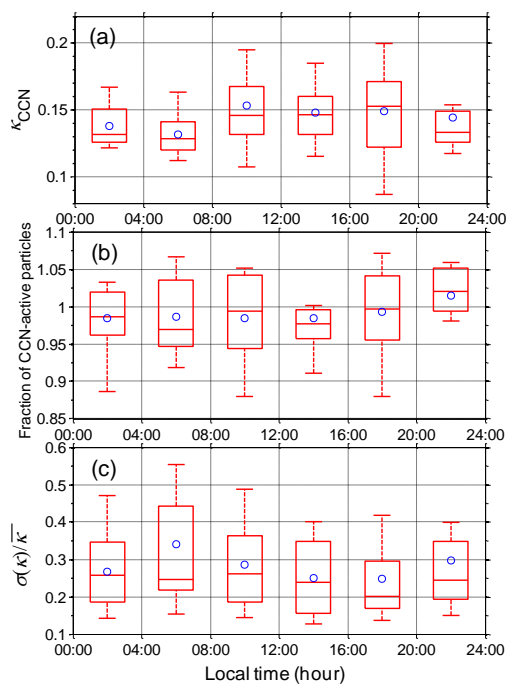


Fig. 5. The diurnal variations of **(a)** the average hygroscopicity, **(b)** maximum activation fraction, and **(c)** dispersion of size-selected CCN active particles ranging from 100 to 171 nm. The ends of the whiskers represent the minimum and maximum of data expect for the outlines, which are defined as points outside of $\pm 2.7\sigma$. The bottom and the top of the box are the 25th and 75th percentiles, the line inside the box is the 50th percentile, and the blue circle represents the mean value.

9396

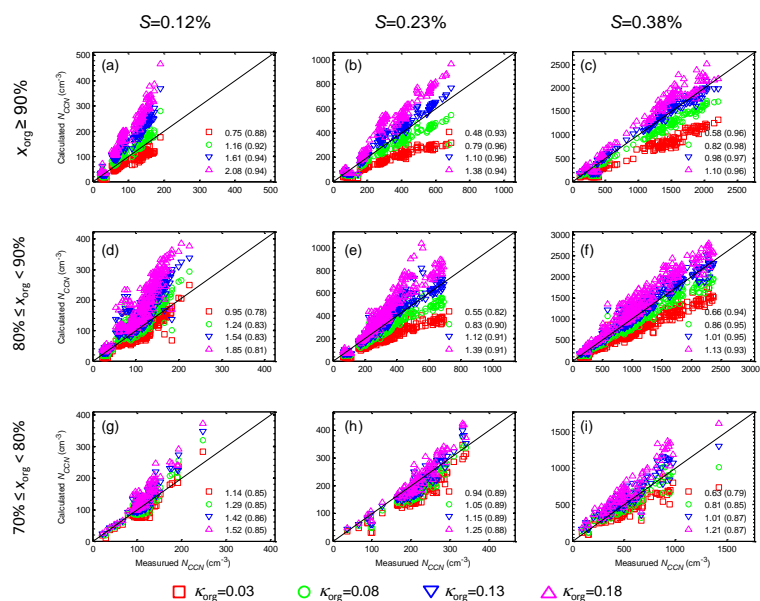


Fig. 6. Comparison of N_{CCN} calculated using four different κ_{org} values and the measurements at supersaturations of 0.12% (**a**, **d**, and **g**), 0.23% (**b**, **e**, and **h**), and 0.38% (**c**, **f**, and **i**) for cases when $x_{\text{org}} > 90\%$ (**a**, **b**, and **c**), $80\% < x_{\text{org}} < 90\%$ (**d**, **e**, and **f**), and $70\% < x_{\text{org}} < 80\%$ (**g**, **h**, and **i**). The slope (left, derived through a bivariate least squares fit) and the R^2 value (in the parenthesis) are shown for all assumed κ_{org} values in each plot.

9397

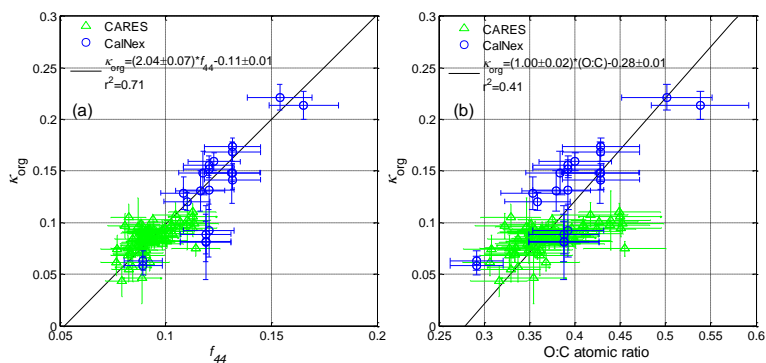


Fig. 7. Derived κ_{org} as a function of **(a)** f_{44} and **(b)** O : C atomic ratio and least squares fits.

9398

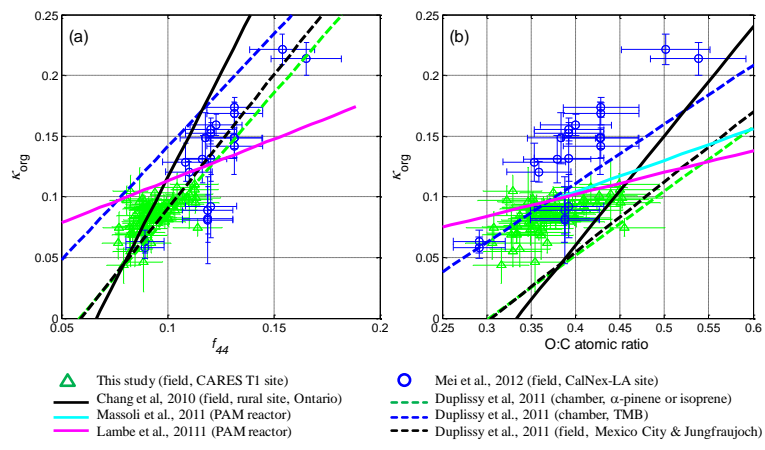


Fig. 8. Comparison with earlier studies on **(a)** the variation of κ_{org} with f_{44} and **(b)** the variation of κ_{org} with O : C. The solid and dashed lines represent κ_{org} derived under supersaturated and subsaturated conditions in earlier studies, respectively.